Ceiling-mounted occupancy detection

using XENSIV™ DEMO BGT60TR13C 60 GHz radar

About this document

Scope and purpose

This application note describes the waveform, signal processing chain, and hardware setup details for segmenting and tracking human targets in a 360-degree field of view (FoV) using the 60 GHz frequency modulated continuous waveform (FMCW) XENSIV™ BGT60TR13C radar sensor.

The focus of this application is on processing the raw data from the sensor to obtain 2D information (X, Y) that corresponds to the target's position relative to the sensor in a 360-degree field of view. A visualization of the target segmentation in each of the four quadrants is provided based on the recorded data from the sensor, which is mounted on the ceiling.

Intended audience

This document is intended for design engineers, technicians, and developers of electronic systems who are interested in developing a use case scenario for target detection and tracking using FMCW technology. The focus of this document is on using the FMCW technology to detect people within a 360-degree field of view when such a sensor is mounted in the ceiling.

Table of contents

1 Introduction

Radar technology has come a long way in recent years, providing an array of powerful solutions that can be integrated into a variety of smart home applications. Whether it is mounted in the ceiling of a room or located in a different area altogether, radar can detect a person's presence and trigger the activation of smart lights, fans, and other devices, providing a convenient and efficient way to enhance your home's automation capabilities. In this application note, Infineon's 60 GHz mmWave BGT60TR13C radar sensor is utilized for occupancy detection performance when mounted in the ceiling of a room.

Besides, the angular tracking capability of the radar can also be used to realize more advance use cases such as defining zones of detection and subsequently trigger an event, just like zones of detection are defined for video doorbells to prevent unnecessary notifications. Similarly, an application can also be realized in an industrial environment where the radar sensor is mounted in the ceiling and covers the perimeter around the working robot. The radar can be used to warn the user if it comes near the vicinity of the robot.

1.1 BGT60TR13C MMIC

BGT60TR13C is a compact, multichannel FMCW radar MMIC that offers one transmitter and three receiver antennas. The chip measures 5 mm x 6.05 mm x 0.8 mm package and includes an integrated state machine that ensures the overall radar system operates efficiently by placing the chip into different power modes to reduce power consumption. The integrated receiver antennas are organized in an L-shape to detect the angle of the target in both the azimuth and elevation plane, as shown in Figure 1. For more information, see the datasheet [1].

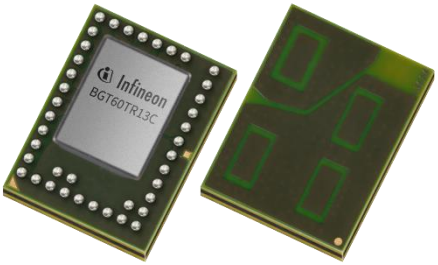

Figure 1 BGT60TR13C radar transceiver

Infineon offers a demo board called "Radar Baseboard MCU7" that hosts the BGT60TR13C radar chip and a microcontroller. The DEMO BGT60TR13C board [3] is shown in Figure 2. The microcontroller collects raw ADC data from the BGT60TR13C radar via the SPI interface and transfers it to the host/PC via the USB interface. The SPI interface runs at 50 MHz and the USB interface supports a high-speed rate of 480 Mbit/s. The collected data from the BGT60TR13C is then processed in MATLAB on the host to derive the range, angle, and velocity of the target.

For more information on the implementation of the communication protocol, see the documentation provided in the Infineon Radar Development Kit (RDK). The RDK is available in the Developer Center Launcher from Infineon [2].

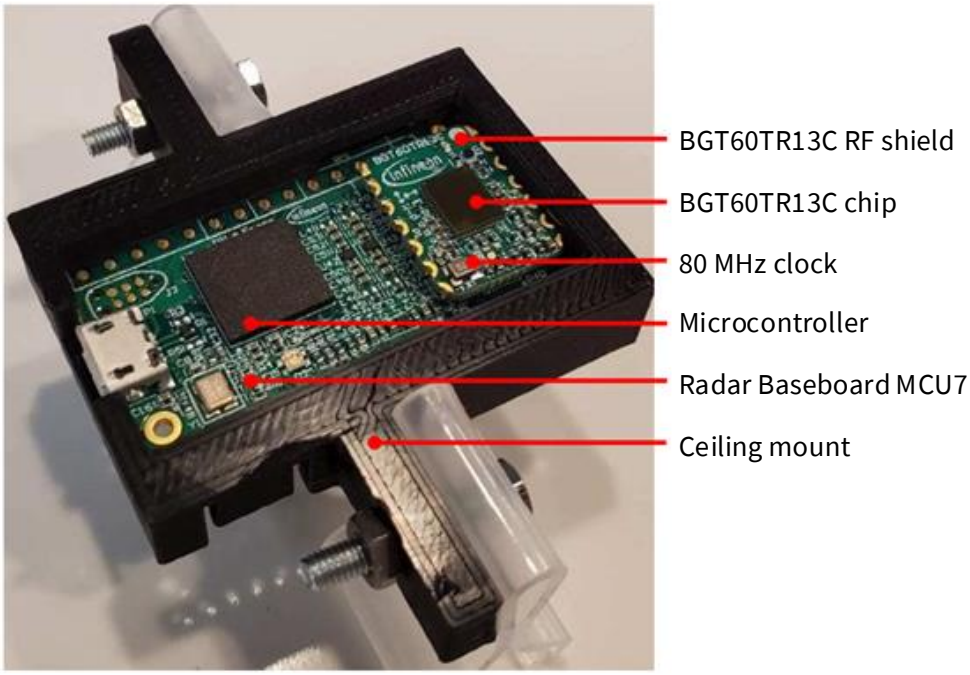

Figure 2 DEMO BGT60TR13C board with ceiling mount

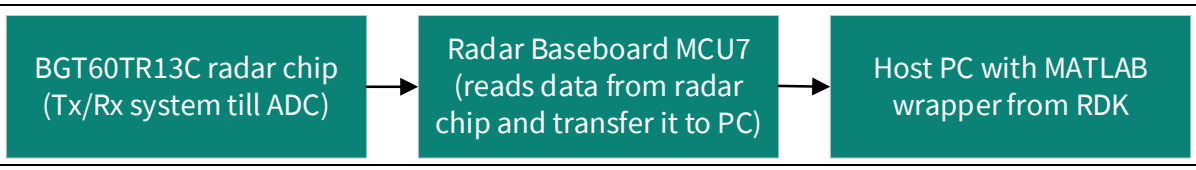

Figure 3 BGT60TR13C to capture raw data

For occupancy sensing within a room, the use case requires the detection of human targets within a room size of up to 6 m x 6 m when the sensor is mounted on the ceiling. The human targets could be either moving or standing still. In recording, the ceiling height is 3.6 m, as shown in Figure 4.

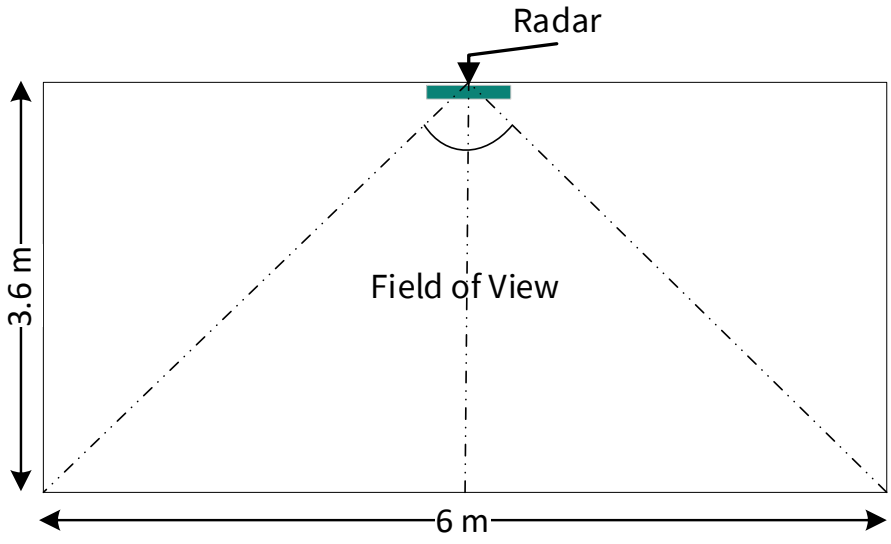

Figure 4 DEMO BGT60TR13C board mounted in the ceiling of a room

1.2 Device parameters

Table 1 Radar waveform configuration details

Parameter	Value
Start/stop frequency	61.02–61.48 GHz
Samples per chirp	128
ADC sample rate	2 MHz
Chirp repetition time	0.314 msec
Frame repetition time	150.1 msec
Number of chirps per frame	64
Bandwidth	460 MHz
Rx antennas	[1, 2, 3]
Tx power level	DAC set to 31 (~+10 dBm)

To ensure that the sensor can be operated in the ISM band (61–61.5 GHz) which is available in most parts of the world, consider a 460 MHz modulated bandwidth configuration. The waveform configuration described above corresponds to a range resolution value of 0.32 m and a Doppler resolution value of 0.12 m/s.

1.3 Test setup and data collection

The DEMO BGT60TR13C board from Infineon is positioned at the heart of the 360-degree visual field, surveying a test area measuring 6 m x 6 m. The origin is defined at the core of the region, where the subject is situated. Each quadrant is assigned a number from 1 to 4, following a clockwise sequence. The sensor is installed at an elevation of 3.6 m above the ground and is firmly attached to the ceiling, as shown in Figure 4. Its location coincides with the center of the field of view. Furthermore, a pair of cameras are strategically mounted on the ceiling to record video footage.

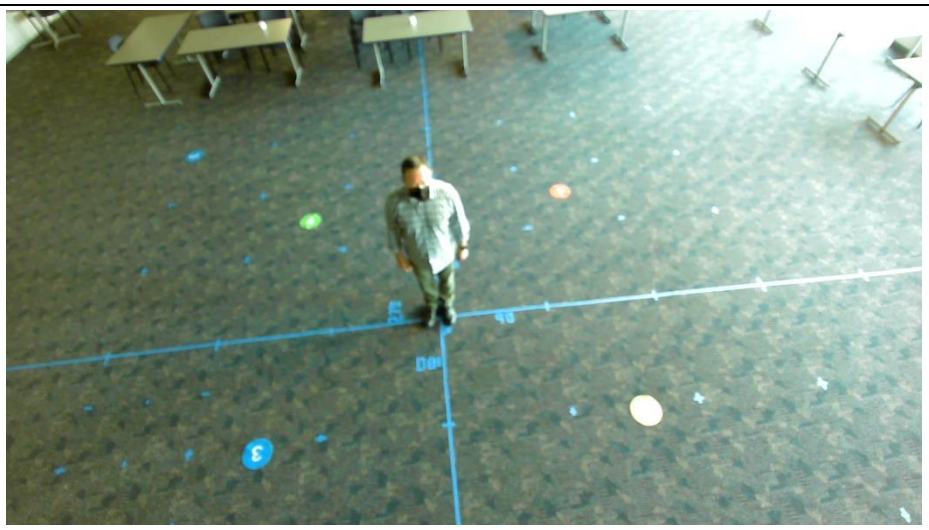

Figure 5 Radar sensor and camera placement on ceiling for 360-degree field of view

To build the fixture and attach it to the ceiling, a CAD model for the DEMO BGT60TR13C board is 3D printed. Figure 6 shows the fixture mounted at a height of 3.6 m on the ceiling.

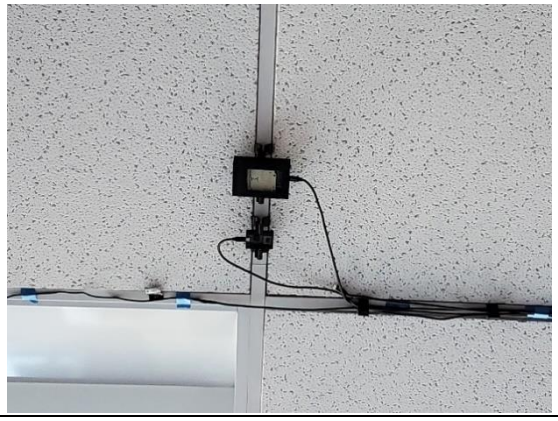

Figure 6 DEMO BGT60TR13C board fixture on the ceiling

Note: Note that the test setup shows two fixtures, but only the fixture that fits the board is used. It is crucial to remember that during testing, the antennas are oriented in the same way as shown in Figure 6.

The BGT60TR13C radar sensor is flipped so that the array normal points towards the ground when mounted on the ceiling. The Rx3 position is defined as the reference origin. The direction from Rx3 to Rx1, representing the H-plane of the array is defined as the X-axis or horizontal direction. Similarly, the direction from Rx3 to Rx2, representing the E-plane of the array is defined as the Y-axis or vertical direction.

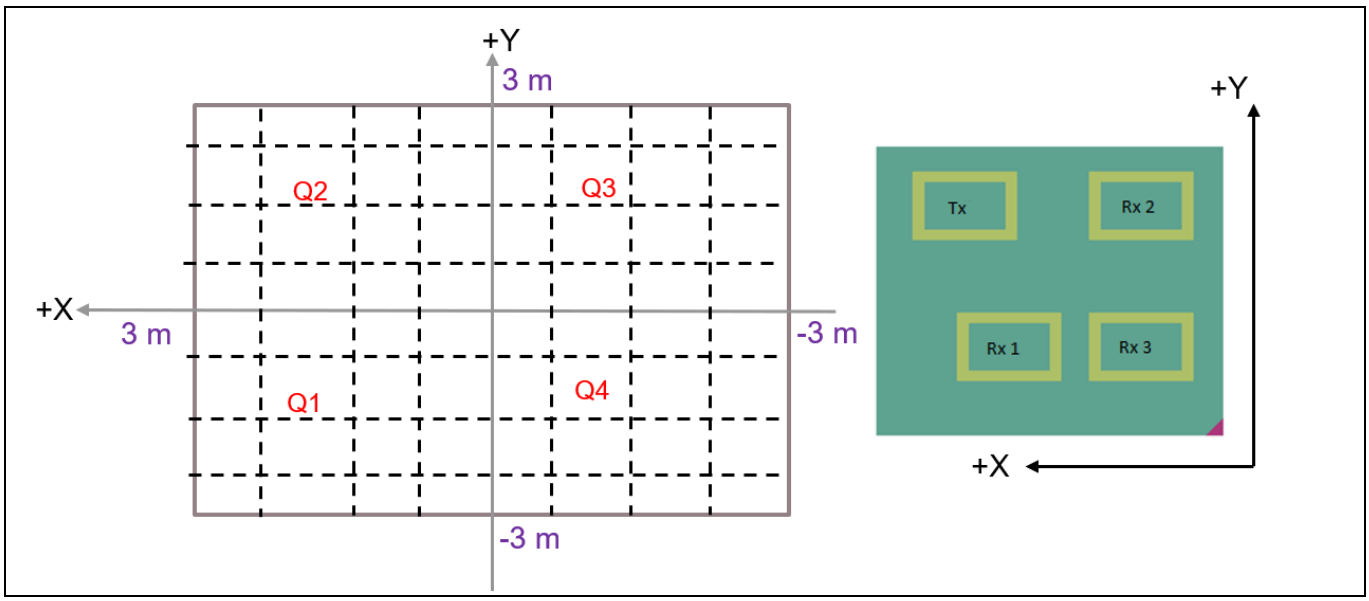

Figure 7 Illustration of BGT60TR13C radar orientation details within the testing region

The grid on the left measures 1 m x 1 m and the area of interest is [-3, 3] m in both the X and Y directions. The right shows the antenna array details from a top view after the chip has been flipped and is pointing towards the ground.

Raw data is collected at every grid point as shown in Figure 6, within the range of [-3, 3] m at 1 m spacing. At each point, the subject remains still for approximately 15 s. To simplify the data collection procedure and gather data from multiple grid points simultaneously, data is collected per quadrant and per row (X-direction in Figure 6). There are a total of four quadrants and each quadrant has four rows (at 0 m, 1 m, 2 m, and 3 m).

Consequently, 16 datasets were captured in total. Each row is collected for nearly 440 frames as the subject walks along the row, starting from Y = 0, and remains still at each meter for 15 s.

To collect the raw data from the board via USB to a PC, the MATLAB wrapper from the Radar SDK [2] and Radar Baseboard MCU7 firmware binary image are utilized. The processing chain is developed in MATLAB software, allowing the collected raw data to be captured and processed offline.

2 Radar signal processing chain

This section delves into the fundamental building blocks of the radar data processing pipeline, specifically for segmentation and tracking applications in 2D (x, y) coordinates, based on the ceiling mount test setup described in the previous section. The algorithm flow detailed in this document support 2D angle of arrival (AoA) processing.

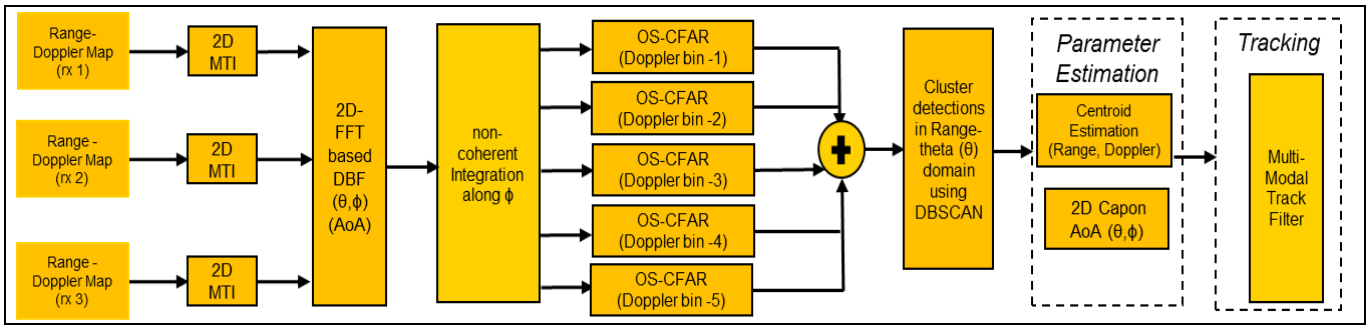

Figure 8 Signal processing pipeline for segmentation and tracking in 2D (x, y) for ceiling mount-based radar

2.1 Input raw data

The input for the signal processing pipeline, as shown in Figure 7, comes in the form of a 3D raw data matrix. This matrix characterized by its dimensions (samples_per_chirp x number_of_chirps x nchannels) is measured at the ADC output of the radar device. It collects data from all the three Rx channels for each frame.

2.2 Range Doppler FFT

To detect and estimate the range of the target, the raw ADC data is normalized to values between [-1, 1]. A window-based fast fourier transform (FFT) operation is then performed on the samples for each chirp. A Blackman window is applied to reduce side lobes and enhance the signal-to-noise (SNR) of the real signal, which is the signal aimed to extract. Subsequently, a column-wise Fourier transform is executed over the second dimension, the slow time, i.e., across all chirps for each sample. This process estimates the Doppler speed and direction of the target. This entire 2D Range Doppler FFT operation can be performed simultaneously on all three receiver channels.

2.3 2D moving target indication filter

The radar returns from static targets such as furniture or metallic poles within the field of view; remove such objects to obtain accurate information about the actual targets in the FoV. The moving target indicator (MTI) filter facilitates this process. The MTI filter, an exponential filter is applied to the Range-Doppler Images obtained from the first step. The main goal of this process is to perform exponential filtering across the Range-Doppler Images in consecutive frames, eliminating returns from completely static targets. Returns from static targets do not vary over time, and so they can be removed.

The Range-Doppler image at time instance 0 is denoted by x_0. This image is then used for filtering for all time steps that are greater than 0. The filter coefficient α, which lies between 0 and 1, is set to 0.3 for this particular application.

$$s_0 = x_0$$

$$s_t = \alpha x_t + (1-\alpha)s_{t-1}$$

Equation 1

2.4 2D FFT-based digital beamforming (DBF)

Digital beamforming is performed across the spatial/Rx channels, which is the third dimension in the raw data matrix to estimate the spatial spectrum across an angular grid. In the case of the BGT60TR13C radar, as the Rx antennas are arranged in an L-shaped pattern, the spatial spectrum can be estimated in both directions along which Rx13 and Rx23 channels are aligned. To achieve this, rearrange the 3D data output from the 2D MTI as a 4D matrix. Here, the third dimension includes channels from Rx1 and Rx3, while the fourth dimension includes channels from Rx2 and Rx3.

Define your coordinate system with Rx3 channel serving as the reference element and origin. The position vector for the remaining two Rx antennas, in x, y, and z coordinates, is defined as follows:

$$\overrightarrow{Rx_1} = \left[\frac{\lambda}{2}\ 0\ 0\right] \rightarrow [d_x\ 0\ 0]$$

$$\overrightarrow{Rx_2} = \left[0\ \frac{\lambda}{2}\ 0\right] \rightarrow [0\ d_y\ 0]$$

$$\overrightarrow{Rx_3} = [0\ 0\ 0]$$

Equation 2

Where,

$d_x = d_y = \frac{\lambda}{2}$ = Distance between the Rx antenna element and the reference Rx element in both x and y directions as a function of wavelength. Furthermore, cartesian coordinates (x, y) are defined as follows:

$$\mathrm{x} = \mathrm{r}\cos\theta\cos\varphi$$

$$y = \mathrm{r}\sin\varphi$$

Equation 3

A steering or weight vector, denoted as ($w(\theta, \phi)$), is defined in the following way so that appropriate phase shifts can be introduced to steer the beam in direction of $\vec{k}$.

$$w(\theta,\phi) = [e^{j\vec{k}.\overrightarrow{D_1}}\ \ e^{j\vec{k}.\overrightarrow{D_2}}\ e^{j\vec{k}.\overrightarrow{D_3}}]$$

$$\vec{k} = \frac{2\pi}{\lambda}[\cos\theta\cos\phi \qquad \sin\phi]$$

Equation 4

Where,

$\vec{k}$ = Wave number vector with angles θ and ϕ respectively in X and Y direction.

$\overrightarrow{D_1}, \overrightarrow{D_2}, \overrightarrow{D_3}$ = Position vector of the Rx antenna array elements, $\overrightarrow{Rx_1}, \overrightarrow{Rx_2}, \overrightarrow{Rx_3}$ from the origin.

By substituting and calculating the dot product between both $\vec{k}$ and $\overrightarrow{D_l}$ vectors in the above equation, it is defined by the weight vector as follows:

$$w(\theta, \phi) = [\ e^{j\frac{2\pi}{\lambda}(d_x \cos\theta \cos\phi)}\ \ e^{j\frac{2\pi}{\lambda}(d_y \sin\phi)}\ \ 1\ ]$$

Equation 5

Compute this weight vector along the grid of $\theta \in [0°, 180°]$ and $\phi \in [-90°, 90°]$ to span the X-Y plane.

The multiplication of the weight vector with the Range Doppler value from each Rx channel (z_m) and the summation of the output is equivalent to delay and sum beamforming/digital beamforming technique (DBF).

$$P(\theta, \phi) = \sum_{m=1}^{M} z_m w(\theta, \phi)$$

Equation 6

For an antenna array with uniform spacing, this operation is equivalent to a discrete Fourier transform and it can be computed using an FFT operation for each spatial dimension. The result of this processing chain is a 4D matrix with the dimensions equivalent to NRng x NDop x NAz x Nel.

2.5 Detection (non-coherent integration and OS-CFAR)

The 2D FFT-based angle of arrival (AoA) step outputs a 4D matrix. To select the range and theta values of the target, first perform non-coherent integration, i.e., sum the amplitude values along the fourth dimension (the second angular grid sampled from the Rx23 channel direction - ϕ). This process creates a 3D matrix equivalent to NRng × NDop × NumTheta.

In the subsequent step, generate range-theta maps for the five highest SNR Doppler responses. Calculate the SNR across each Doppler grid and sort it in descending order. Then, apply the Order Statistic Constant False Alarm Rate (OS-CFAR) detection technique to each of the Range-theta maps to detect range-theta pairs that exceed the detector threshold. The threshold set in the OS-CFAR is an adaptive value estimated from the neighboring grid values, aiming to achieve a user-defined false alarm rate. For more details related to this algorithm, see [4]. In this approach, non-coherent integration is performed along the ϕ direction instead of coherent integration.

The range-theta pair values selected from each of the five Doppler bins are then accumulated to create a range-theta map.

2.6 Clustering (DBSCAN)

The range-theta values that passed the detection threshold in the previous section are inputted into a clustering algorithm block, known as density-based spatial clustering of applications with noise (DBSCAN). Human targets tend to be spread over multiple ranges and theta bins. As such, it becomes necessary to cluster or group together the target detections into a single target point cluster.

2.7 Parameter estimation

This block is employed to estimate the range (r), theta (θ), phi (ϕ), and radial velocity of the centroid of the points that are grouped together by the DBSCAN algorithm.

2.7.1 Range estimation

The Doppler index is computed by deriving the maximum value from all the values for the estimated range index. This Doppler index is then used to estimate the Doppler velocity of the targets, as follows:

$$\text{Range (m)} = (\text{Range index-1}) \text{ x Distance per range bin}$$

Equation 7

Where,

Distance per range bin = $\frac{c_0}{2\,B}$

c_0 = Speed of light in vacuum (m/s)

B = Bandwidth (Hz)

2.7.2 Doppler estimation

The Doppler index is computed by obtaining the maximum over all the values for the estimated range index. This Doppler index is used to estimate the Doppler velocity of the targets as follows:

$$\text{Radial Velocity (m/s)} = (\text{Doppler index} - (\frac{\text{Doppler FFT size}}{2}) - 1)) \text{ x Doppler resolution x } \frac{c\_0}{2f_c}$$

Equation 8

Where,

c_0 = Speed of light in vacuum

f_c = Center frequency

2.7.3 Theta and Phi estimation

To estimate the AoA of the centroid of the detections, a direction of arrival technique known as 2D Capon technique [5] is applied on the estimated range cell data collected from all the three Rx channels. Consider 2D Capon instead of DBF to improve the resolution of the estimated value.

For each range (r), estimated in Section 2.7.1, select the Doppler bin index of the maximum Range-Doppler output from the Rx3/reference channel. From this specific range-Doppler pair value, select the neighboring bins/snapshots along the Doppler dimension to estimate the covariance matrix (R). The power spectrum for the capon angle of arrival algorithm is as follows:

$$P(\phi) = w(\phi)^H R^{-1} w(\phi)$$

Equation 9

The power spectrum obtained using this technique improves the angular resolution of high SNR targets [5].

For 2D AoA estimation along θ and ϕ, first process the input data from Rx2 and Rx3 channels to estimate power spectrum at ϕ. To achieve this, define the steering or weight vector along the Rx32 channel direction as follows:

$$w(\phi) = [\ \ 1 \ \ \ e^{j\frac{2\pi}{\lambda}(d_y \sin\phi)}\ \ ]$$

Equation 10

Note: Included an additional phase offset of 30° in Rx23 channel direction that is obtained after array calibration and the power spectrum value is calculated across the $\phi \in$ [-90°, 90°] with 4° bin size.

The index of the maximum $P(\phi)$ value corresponds to the estimated $\hat{\phi}$ value of the target. In the second step, estimate the $\hat{\theta}$ for the above-estimated $\hat{\phi}$ value by processing the data from Rx1 and Rx3 channels, while considering the weight vector as follows:

$$w(\theta, \phi) = [\ \ e^{j\frac{2\pi}{\lambda}(d_x \cos\theta \cos\hat{\phi})} \ \ \ 1\ ]$$

Equation 11

At the conclusion of the parameter estimation block, a list of detected targets/target measurements is generated. Each item on this list comes with its respective parameter estimates – range (r), theta (θ), phi (ϕ), and speed value of the centroid.

2.8 Tracking

Apply an interacting multi-modal (IMM) filter, to track the range (r), theta (θ), and Doppler speed values from frame-to-frame. To track and update the elevation, implement an additional alpha-beta filter. The prediction and correction filter equations for the alpha-beta filter are provided in [6].

2.9 Visualization and the application output

In the last step, the tracked range (r), theta (θ), and phi (ϕ) values are converted to cartesian coordinate system (x, y) based on the following equations. Combine the tracker output data collected from all four rows per each quadrant and overlay detections from all of the four quadrants in a single plot to obtain the presence/occupancy grid as discussed in the next section.

$$\mathrm{x} = \mathrm{r}\cos\theta\cos\varphi$$

$$y = \mathrm{r}\sin\varphi$$

Equation 12

3 Data processing

The raw data from the recordings is first processed based on the presence detection algorithm available in RDK [2]. The presence detection algorithm in RDK version considers single Rx channel data and Range Doppler output with a hard thresholding technique to determine presence (1) or absence (0). See the SDK documentation for full algorithm details [2]. The result obtained from Rx channel 3 is shown in Figure 9. It obtains full coverage in X-dimension of 6 m range for y = 0 and 1 m.

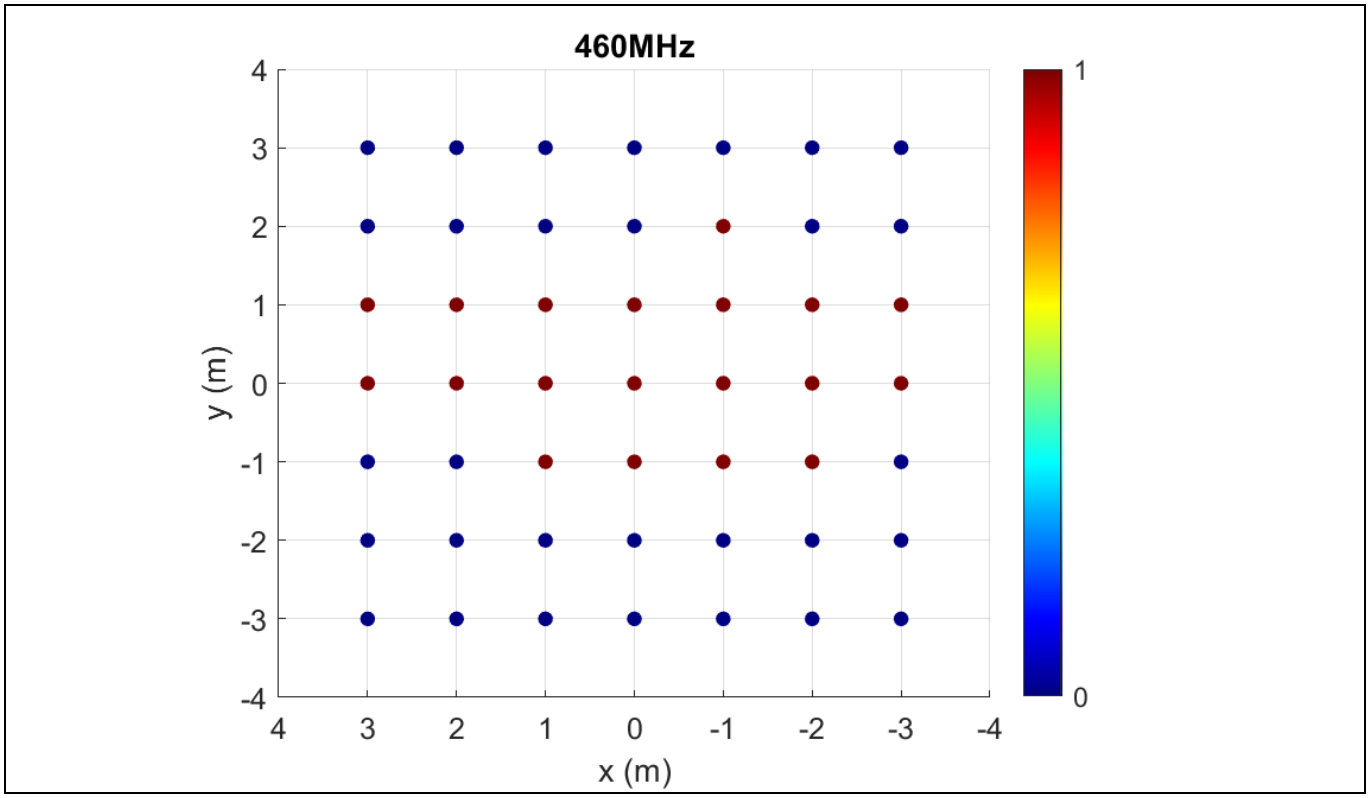

Figure 9 Output of presence detection algorithm from RDK with threshold value set to 0.0005

In Figure 9, red (1) indicates that presence is detected, while blue (0) implies that no presence is detected despite the subject being present.

Furthermore, the raw data is processed based on the signal processing chain described in Section 2. Figure 9 and Figure 10 display the result after combining the output from all the datasets that were collected in each quadrant. A subplot is created for each Y-axis to visualize the offset between the true and estimated Y-value (i.e., along the Rx23 channel direction). It is observed that the accuracy of the estimated x and y values degrades at the edge of the field of view, specifically at 3 m in the positive and negative directions of both x and y axes.

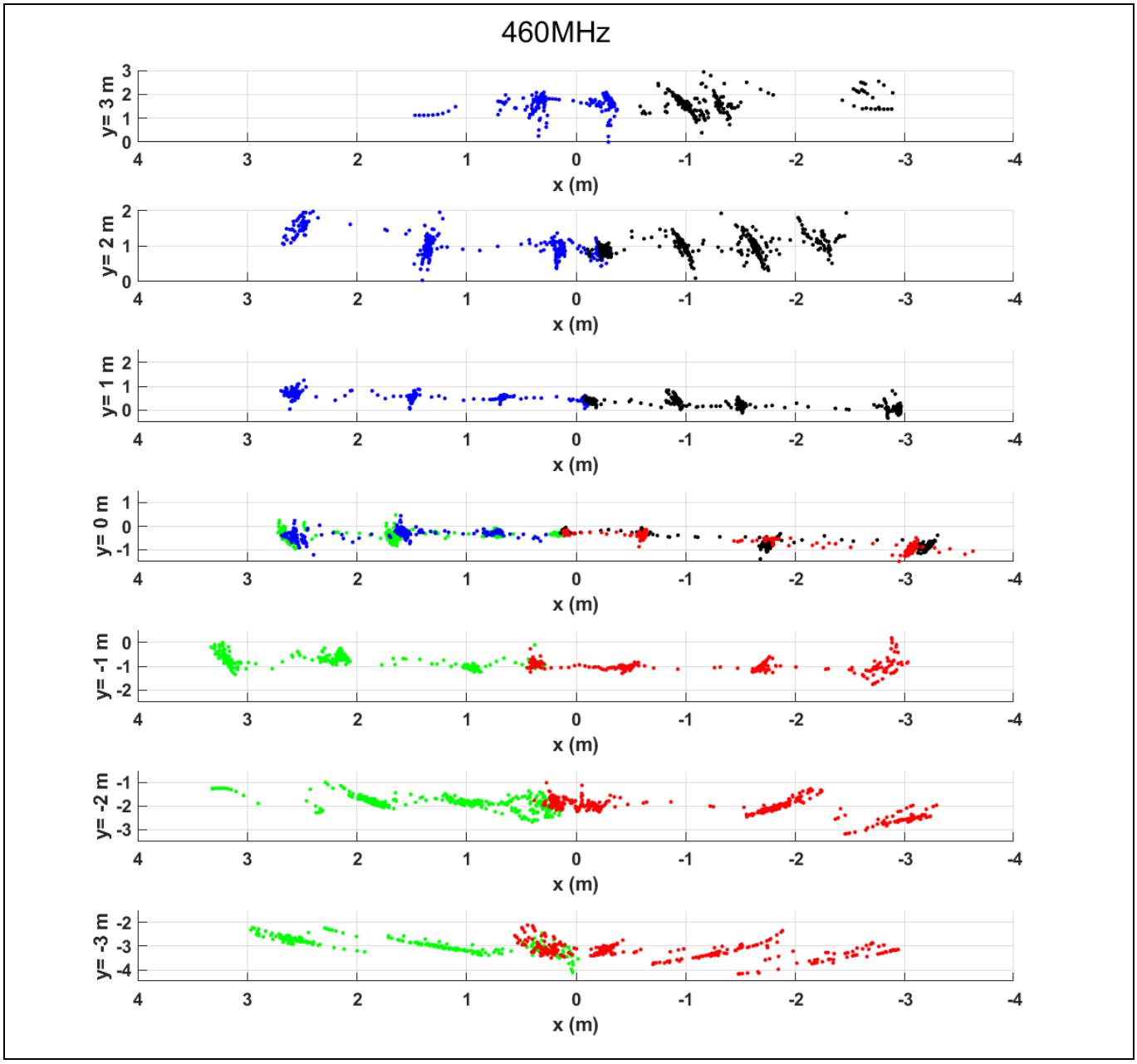

Figure 10 Output of the radar signal processing chain

Figure 10 displays the estimated x and y values obtained from the dataset collected within a range of [-3, 3] m in both X and Y directions. The data corresponds to a single individual standing still at every 1 m spacing for 15 s.

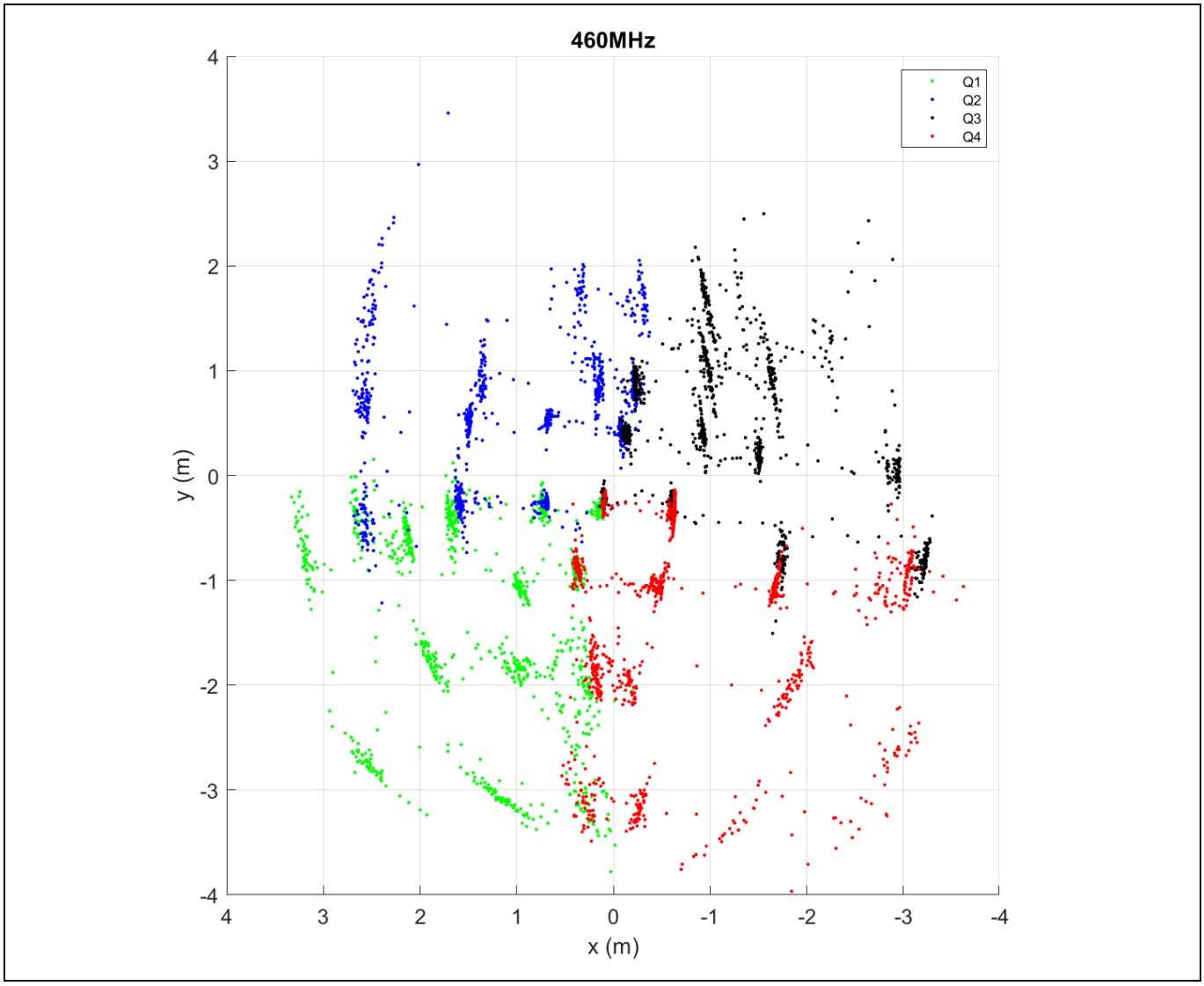

Figure 11 Combined plot of results

The different colors (green, blue, black, and red) in Figure 11 represent the estimates obtained from each respective quadrant (Q1, Q2, Q3, and Q4) respectively.

4 Summary

In summary, this document details the waveform configuration, mounting setup, data collection, and signal processing flow necessary to detect targets from a ceiling-mounted BGT60TR13C radar sensor. This radar comprises an L-shaped array in both the X and Y dimensions. Measurements are obtained from the sensor, which is mounted at a height of 3.6 m. Process the results using both the presence detection application available in the Radar Development Kit (RDK), which is based on Range-Doppler using a single Rx channel processing technique and the 2D angle of arrival (AoA) processing chain described in Section 2.

Based on the test data collected, managed to detect presence in the Y-axis within the range of [-1, 1] m. With the 2D AoA processing technique, extended this range to [-3, 1] m with an accuracy in the range of 2 m along the E-plane direction (Rx23, Y-axis) of the array.

Consideration

In this situation, the sensor has been placed at a height of 3.6 meters due to setup restrictions, which is higher than the typical ceiling height of 2.75 meters. However, it is still achievable to obtain a wider area of ground coverage in a scenario with a ceiling height of 2.75 meters.

References

[1] Infineon Technologies AG: *BGT60TR13C datasheet;* Available online

[2] Infineon Technologies AG: *Radar Development Kit (RDK)*; Available online

[3] Infineon Technologies AG: *DEMO BGT60TR13C;* Available online

[4] Mark A. Richards, *Fundamentals of Radar Signal Processing*, McGraw-Hill, 2014.

[5] Harry L. Van Trees, *Optimum Array Processing: Part IV of Detection, Estimation, and Modulation Theory*, John Wiley & Sons, 2004.

[6] A. Santra and S. Hazra, *Deep Learning Applications of Short-Range Radars*, Artech House, 2020.

Revision history

Document revision	Date	Description of changes
1.00	2024-02-15	Initial release

Trademarks
All referenced product or service names and trademarks are the property of their respective owners.

Edition 2024-02-15

Published by

Infineon Technologies AG

81726 Munich, Germany

Do you have a question about this document?

Email: erratum@infineon.com

Document reference

AN141319

Important notice

The information contained in this application note is given as a hint for the implementation of the product only and shall in no event be regarded as a description or warranty of a certain functionality, condition or quality of the product. Before implementation of the product, the recipient of this application note must verify any function and other technical information given herein in the real application. Infineon Technologies hereby disclaims any and all warranties and liabilities of any kind (including without limitation warranties of non-infringement of intellectual property rights of any third party) with respect to any and all information given in this application note.

The data contained in this document is exclusively intended for technically trained staff. It is the responsibility of customer's technical departments to evaluate the suitability of the product for the intended application and the completeness of the product information given in this document with respect to such application.

Warnings

Due to technical requirements products may contain dangerous substances. For information on the types in question please contact your nearest Infineon Technologies office.

Except as otherwise explicitly approved by Infineon Technologies in a written document signed by authorized representatives of Infineon Technologies, Infineon Technologies' products may not be used in any applications where a failure of the product or any consequences of the use thereof can reasonably be expected to result in personal injury.